

# Lawrence Berkeley National Laboratory

## Lawrence Berkeley National Laboratory

### Title

Influence of Bottom Quark Jet Quenching on Single Electron Tomography of Au+Au

### Permalink

<https://escholarship.org/uc/item/24x656sm>

### Authors

Djordjevic, Magdalena

Gyulassy, Miklos

Vogt, Ramona

et al.

### Publication Date

2005-07-12

Peer reviewed

# Influence of Bottom Quark Jet Quenching on Single Electron Tomography of Au+Au

Magdalena Djordjevic,<sup>1</sup> Miklos Gyulassy,<sup>1</sup> Ramona Vogt,<sup>2</sup> and Simon Wicks<sup>1</sup>

<sup>1</sup>*Department of Physics, Columbia University, 538 West 120-th Street, New York, NY 10027*

<sup>2</sup>*Nuclear Science Division, LBNL, Berkeley, CA 94720 and Physics Department,  
University of California, Davis, California 95616*

(Dated: July 21, 2005)

High transverse momentum single (non-photonic) electrons are shown to be sensitive to the stopping power of both bottom,  $b$ , and charm,  $c$ , quarks in  $AA$  collisions. We apply the DGLV theory of radiative energy loss to predict  $c$  and  $b$  quark jet quenching and compare the FONLL and PYTHIA heavy flavor fragmentation and decay schemes. We show that single electrons in the  $p_T = 5 - 10$  GeV range are dominated by the decay of  $b$  quarks rather than the more strongly quenched  $c$  quarks in Au+Au collisions at  $\sqrt{s} = 200$  AGeV. The smaller  $b$  quark energy loss, even for extreme opacities with gluon rapidity densities up to 3500, is predicted to limit the nuclear modification factor,  $R_{AA}$ , of single electrons to the range  $R_{AA} \sim 0.5 - 0.6$ , in contrast to previous predictions of  $R_{AA} \lesssim 0.2 - 0.3$  based on taking only  $c$  quark jet fragmentation into account.

PACS numbers: 12.38.Mh; 24.85.+p; 25.75.-q

## Introduction.

Recent data [1] from the Relativistic Heavy Ion Collider (RHIC) on “perfect fluidity” [2]-[5] and light quark and gluon jet quenching [6]-[9] provide direct evidence that a novel form of strongly interacting Quark Gluon Plasma (sQGP) is created in central Au+Au collisions at  $\sqrt{s} = 200$  AGeV [10].

In the near future, measurements of heavy quark jet quenching will provide further important tests of the transport properties of this new form of matter. In particular, rare heavy quark jets are valuable independent probes of the intensity of color field fluctuations in the sQGP because their high mass ( $m_c \approx 1.2$  GeV,  $m_b \approx 4.75$  GeV) changes the sensitivity of both elastic and inelastic energy loss mechanisms in a well defined way [11]-[17] relative to those of light quark and gluon jets [6]-[9]. Open heavy quark meson ( $D$ ,  $B$ ) tomography also has the unique advantage that - unlike light hadron ( $\pi$ ,  $K$ ) tomography that is sensitive to the large difference between quark and gluon energy loss - gluon jet fragmentation into  $D$  and  $B$  mesons can be safely neglected.

The “fragility” of light hadron tomography pointed out in Ref. [18] is primarily due to the significant reduction in sensitivity of the attenuation pattern to the sQGP density when the gluon jets originating from the interior are too strongly quenched. In that case, the attenuation of light hadrons becomes sensitive to geometric fluctuations of the jet production points near the surface “corona”.

Heavy quarks, especially  $b$  quarks, are predicted to be significantly less fragile in the DGLV [12]-[15] theory of radiative energy loss because their energy loss is expected to be considerably smaller. If radiative energy loss is the dominant jet quenching mechanism in the  $p_T \sim 10$  GeV region, then heavy meson tomography could be a more sensitive tomographic probe of the absolute scale of density evolution and the opacity of the produced sQGP.

However, one disadvantage of heavy meson tomography is that direct measurements of identified high  $p_T$   $D$  and  $B$  mesons are very difficult with current detectors

and RHIC luminosities [19]. Therefore, the first experimental studies of heavy quark attenuation at RHIC have focused on the attenuation of their single (non-photonic) electron decay products [20]-[23].

Some preliminary data [24]-[25] surprisingly suggest that single electrons with  $p_T \sim 5$  GeV may experience elliptic flow and suppression patterns similar to light partons. We emphasize in this letter that either result would have even greater implications than previously thought about the nature of the produced sQGP. If confirmed in the final analysis, the sQGP would have to be completely opaque to even  $b$  quark jets of  $p_T \sim 10$  GeV, in contradiction to all radiative energy loss estimates so far.

A significant complication of the heavy quark decay lepton measurements is that estimates in Refs. [26, 27] indicated that bottom decay leptons may in fact dominate electrons from charm for  $p_T > 3$  GeV in  $pp$  collisions. In this letter, we show that jet quenching further amplifies the  $b$  contribution to the lepton spectrum and strongly limits the nuclear modification factor of electrons in  $AA$  collisions.

The preliminary electron data [24]-[25] are so surprising that novel jet energy loss mechanisms may have to be postulated [28]-[31]. The elliptic flow of high  $p_T$  heavy quarks can be accounted for, e.g., if the *elastic* cross sections of all partons, including bottom, are assumed to be anomalously enhanced to  $> 20$  mb, far in excess of perturbative QCD predictions, up to at least  $p_T \sim 10$  GeV. While these enhanced cross sections could lead to heavy flavor elliptic flow at the pion level even at high  $p_T$ , they may greatly overestimate the attenuation of light and heavy flavored hadrons [31]-[33].

Given the critical role that single electron tomography of the sQGP may play in the near future, it is especially important to scrutinize the theoretical uncertainties and robustness of current predictions. This is the aim of this letter.

## Theoretical framework.

The calculation of the lepton spectrum includes initial

heavy quark distributions from perturbative QCD, heavy flavor energy loss, heavy quark fragmentation into heavy hadrons,  $H_Q$ , and  $H_Q$  decays to leptons. The cross section is schematically written as:

$$\frac{Ed^3\sigma(e)}{dp^3} = \frac{E_i d^3\sigma(Q)}{dp_i^3} \otimes P(E_i \rightarrow E_f) \\ \otimes D(Q \rightarrow H_Q) \otimes f(H_Q \rightarrow e),$$

where  $\otimes$  is a generic convolution. The electron decay spectrum,  $f(H_Q \rightarrow e)$ , includes the branching ratio to electrons. The change in the initial heavy flavor spectra due to energy loss is denoted  $P(E_i \rightarrow E_f)$ .

The initial heavy quark  $p_T$  distributions are computed at next-to-leading order with the code used in Ref. [34, 35]. We assume the same mass and factorization scales as in Ref. [36], employing the CTEQ6M parton densities [37] with no intrinsic  $k_T$ .

As in Ref. [15], we compute heavy flavor suppression with the DGLV generalization [12] of the GLV opacity expansion [7] to heavy quarks. We take into account multi-gluon fluctuations as in Ref. [8].

The fragmentation functions  $D(c \rightarrow D)$  and  $D(b \rightarrow B)$ , where  $D$  and  $B$  indicate a generic admixture of charm and bottom hadrons, are consistently extracted from  $e^+e^-$  data [38–40]. The charm fragmentation function [40] depends on the parameter  $r$  [41]. We take  $r = 0.04$  for  $m_c = 1.2$  GeV. Bottom fragmentation instead depends on the parameter  $\alpha$  [42] with  $\alpha = 29.1$  for  $m_b = 4.75$  GeV. The fragmentation is done by rescaling the quark three-momentum at a constant angle in the laboratory frame.

The leptonic decays of  $D$  and  $B$  mesons are controlled by measured decay spectra and branching ratios. The spectrum for primary  $B \rightarrow e$  decays has been measured recently [43, 44]. The fit to this data [34] is assumed to be valid for all bottom hadrons. Preliminary CLEO data on the inclusive semi-leptonic electron spectrum from  $D$  decays [45] have also been fitted [34] and assumed to be identical for all charm hadrons. The contribution of leptons from secondary  $B$  decays  $B \rightarrow D \rightarrow e$  is obtained as a convolution of the  $D \rightarrow e$  spectrum with a parton-model prediction for  $b \rightarrow c$  decay [34]. The resulting electron spectrum is very soft, making it a negligible contribution to the total, particularly at  $p_T > 2$  GeV. The appropriate effective branching ratios are [46]:  $B(B \rightarrow e) = 10.86 \pm 0.35\%$ ,  $B(D \rightarrow e) = 10.3 \pm 1.2\%$ , and  $B(B \rightarrow D \rightarrow e) = 9.6 \pm 0.6\%$ .

The uncertainty in our results due to the choice of fragmentation and decay schemes is studied using the corresponding PYTHIA [47] routines, assuming Peterson fragmentation [48] with a range of parameters.

To compute the medium induced gluon radiation spectrum, we need to include in general three effects: 1) the Ter-Mikayelian or massive gluon effect [13, 14], 2) transition radiation [49] and 3) medium-induced energy loss [12, 14]. In Ref. [50], it was shown that first two effects nearly cancel and can thus be neglected for heavy

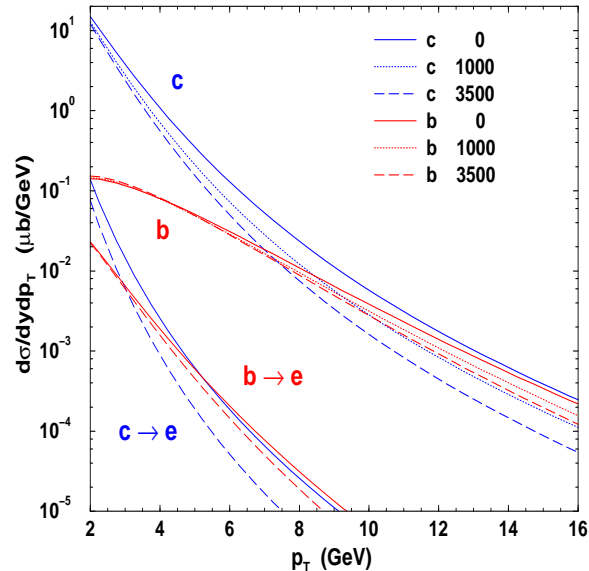


FIG. 1: The differential cross section (per nucleon pair) of charm (upper blue) and bottom (upper red) quarks calculated to NLO in QCD [34] compared to single electron distributions calculated with the fragmentation and decay scheme of Ref. [34]. The solid, dotted and long dashed curves show the effect of DGLV heavy quark quenching with initial rapidity densities of  $dN_g/dy = 0, 1000$ , and  $3500$ , respectively.

quark suppression at zeroth order in opacity. We therefore only compute the medium-induced gluon radiation spectrum [12]. We employ the effective static medium approximation formula

$$\frac{dN_{\text{ind}}^{(1)}}{dx} = \frac{C_F \alpha_s L}{\pi \lambda_g} \int_0^\infty \frac{2\mathbf{q}^2 \mu^2 d\mathbf{q}^2}{\left(\frac{4Ex}{L}\right)^2 + (\mathbf{q}^2 + m^2 x^2 + m_g^2)^2} \\ \times \int \frac{d\mathbf{k}^2 \theta(2x(1-x)p_T - |\mathbf{k}|)}{((|\mathbf{k}| - |\mathbf{q}|)^2 + \mu^2)^{3/2} ( (|\mathbf{k}| + |\mathbf{q}|)^2 + \mu^2)^{3/2}} \\ \times \left\{ \mu^2 + (\mathbf{k}^2 - \mathbf{q}^2) \frac{\mathbf{k}^2 - m^2 x^2 - m_g^2}{\mathbf{k}^2 + m^2 x^2 + m_g^2} \right\}. \quad (1)$$

Here  $E = \sqrt{p_T^2 + m^2}$  is the initial energy of a heavy quark of mass  $m$ ,  $\mathbf{k}$  is the transverse momentum of the radiated gluon and  $\mathbf{q}$  is the momentum transfer to the jet. The opacity of the medium to radiated gluons is  $L/\lambda_g = 9\pi\alpha_s^2/2 \int d\tau \rho(\tau)/\mu^2(\tau)$  where  $\mu \approx g(\rho/2)^{1/3}$  is local Debye mass in a perturbative QGP. The gluon density at proper time  $\tau$  is related to the initial rapidity density of the produced gluons by  $\rho(\tau) \approx dN_g/dy\tau\pi R^2$  with  $R = 6$  fm in central collisions assuming a uniform cylinder undergoing a Bjorken 1+1D expansion. Transverse expansion does not significantly affect the integrated energy loss [51].

The Ter-Mikayelian effect at first order in opacity is due to a asymptotic transverse gluon mass in the medium,  $m_g \approx \mu/\sqrt{2}$ . We assume  $\alpha_s = 0.3$ . The induced radiative energy loss fluctuation spectrum,  $P(E_i \rightarrow E_f)$ , was computed as in Ref. [8], starting from the average

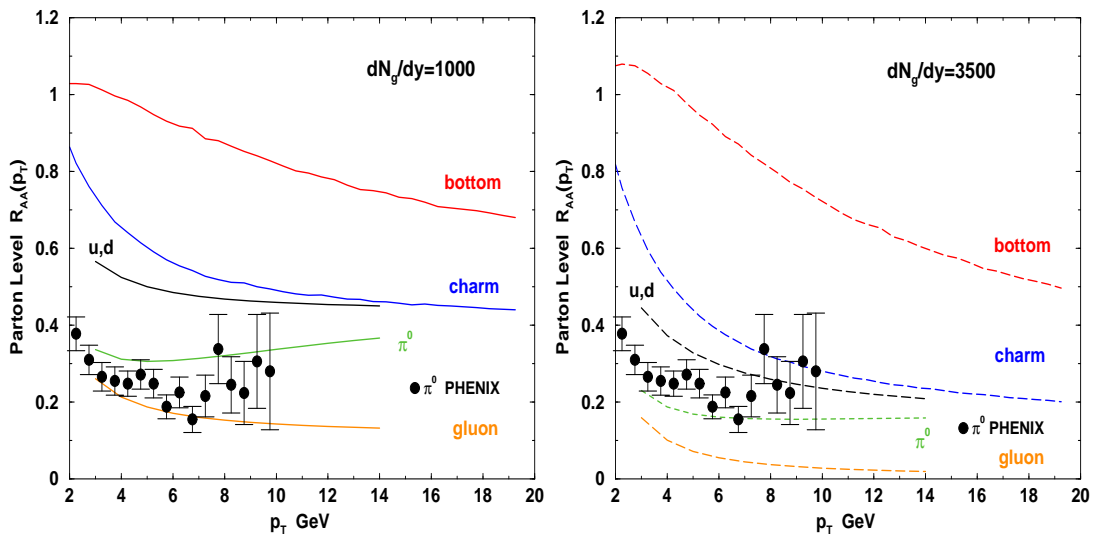


FIG. 2: Heavy quark jet quenching before fragmentation into mesons for  $dN_g/dy = 1000$  (left) and  $3500$  (right) are compared to light ( $u, d$ ) quark and gluon quenching. The resulting  $\pi^0 R_{AA}$  is compared to the central 0-10% PHENIX data [52].

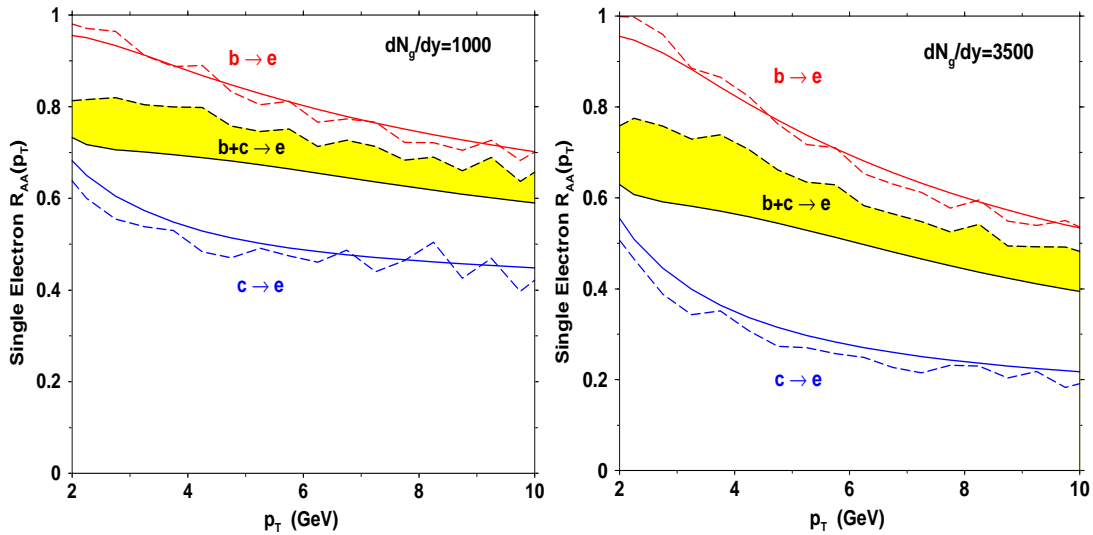


FIG. 3: Single electron attenuation pattern for initial  $dN_g/dy = 1000$ , left, and  $dN_g/dy = 3500$ , right. The solid curves employ the fragmentation scheme and lepton decay parameterizations of Ref. [34] while the dashed curves use the Peterson function with  $\epsilon_c = 0.06$  and  $\epsilon_b = 0.006$  and the decay to leptons employed by the PYTHIA Monte Carlo. Note that even for the extreme opacity case on the right the less quenched  $b$  quark jets dilute  $R_{AA}$  so much that the modification of the combined electron yield from both  $c$  and  $b$  jets does not fall below  $\sim 0.5 - 0.6$  near  $p_T \sim 5$  GeV.

induced gluon spectrum in the effective *static* medium approximation given by Eq (1). In this approximation the effective static  $\rho$  is approximated by  $\rho(\langle\tau\rangle)$  with  $\langle\tau\rangle = R/2 = 3$  fm and  $L = R$ . We have checked that the more numerically intensive Bjorken expansion gives very similar results.

Note that  $k_{\max} = 2x(1-x)p_T$  in Eq. (1) instead of  $k_{\max} = xE$ , as in Ref. [12]. There is a 20% theoretical uncertainty in  $R_{AA}$  due to the range of reasonable kinematic bounds.

### Bottom versus Charm quark suppression

Figure 1 shows the  $c$  and  $b$  quark distributions at midrapidity before fragmentation. The solid curves indicate that, at NLO,  $b$  production becomes comparable to  $c$  production in the vacuum only for  $p_T \gtrsim 15$  GeV. However, jet quenching is greater for the lighter  $c$  quark, and for the default gluon density,  $dN_g/dy = 1000$  [9], the more weakly quenched  $b$ 's dominate over the more strongly quenched  $c$ 's for  $p_T \gtrsim 9$  GeV. For more extreme opacities, characterized here by  $dN_g/dy = 3500$ , the cross

over shifts down to  $p_T \approx 7$  GeV. With the fragmentation and decay scheme of Ref. [34], the electron decay distributions,  $c \rightarrow e$  and  $b \rightarrow e$ , are seen to cross each other at  $p_T \sim 5.5$  GeV when the  $c$  and  $b$  quarks are not quenched, reduced to  $p_T \sim 3$  GeV for  $dN_g/dy = 3500$ . The electron results for  $dN_g/dy = 1000$ , lying between the solid and long-dashed curves in Fig. 1, are not shown for clarity. Thus electrons in the  $p_T \sim 5$  GeV region are sensitive to  $b$  and  $c$  quark quenching.

The parton level quenching is shown in detail in Fig. 2 by the nuclear modification factor,  $R_{AA}(Q) = dN_Q(p_T, dN_g/dy)/dN_Q(p_T, 0)$  with  $Q = g, u, d, c$  and  $b$ . The left-hand side shows results for the default case,  $dN_g/dy = 1000$  [9], while the right-hand side shows the high opacity case,  $dN_g/dy = 3500$ . For comparison, we also show the PHENIX [52] data on the  $\pi^0$  nuclear modification factor measured in the central 0-10% of Au+Au collisions at  $\sqrt{s} = 200$  AGeV. As expected, gluon quenching is largest due to its color Casimir factor and its small in-medium mass. The “dead cone effect” [11] is seen by comparing  $c$  quark quenching to light  $u, d$  quenching at  $p_T < 10$  GeV. For  $p_T > 10$  GeV  $\gg m_c$ , the mass difference between the charm and light quarks is almost negligible [50].

However, in both cases,  $b$  quark quenching remains significantly smaller than that of the light and charm quarks for  $p_T \lesssim 20$  GeV since  $p_T/m_b$  is not large. The effect of the  $b$  mass can therefore never be neglected in the RHIC kinematic range.

Figure 2 also shows an estimate of  $\pi^0$  quenching assuming

$$R_{AA}(\pi^0) \approx f_g R_{AA}(g) + (1 - f_g) R_{AA}(u) , \quad (2)$$

where  $f_g \approx \exp[-p_T/10.5 \text{ GeV}]$  is the fraction of pions with a given  $p_T$  that arise from gluon jet fragmentation. The approximate form is a fit to a leading order QCD calculation at  $\sqrt{s} = 200$  AGeV, discussed in Refs. [53, 54]. The approximation in Eq. (2) is strictly valid only for pure power law gluon and quark distributions with a  $p_T$ -independent spectral index. However, it provides a simple estimate that shows that  $\pi^0$  quenching is primarily controlled by light quark quenching above 10 GeV. In addition, Fig. 2 shows that current data would be incompatible with radiative  $g, u$  and  $d$  quenching if the medium had an opacity greater than that of the  $dN_g/dy = 3500$  case considered on the right-hand side.

We note that the  $c$  quark quenching predicted in Fig. 2 with  $1000 \leq dN_g/dy \leq 3500$  is similar to the quenching range predicted in Fig. 2 of Ref. [17] for the effective transport coefficient  $\hat{q} = \mu^2/\lambda_g$  in the range  $4 \leq \hat{q} \leq 14$  GeV<sup>2</sup>/fm. For a  $c$  quark with  $p_T \sim 12$  GeV, for example, we predict  $R_{AA}(c) \approx 0.25 - 0.5$  in this range, as does Ref. [17] for the same factor of 3.5 variation of the sQGP density.

Our primary new observation is that since  $b$  quark quenching is greatly reduced relative to  $c$  quenching, if heavy quark tomography is performed via single electron suppression patterns, the lower  $b$  quenching strongly lim-

its the possible electron quenching, as we show in Fig. 3. For electrons arising from  $c$  fragmentation and decay, we again confirm the predictions of Ref. [17]. However, for electrons arising from  $b$  decay, there is only a modest amount of quenching. Note the similar magnitudes of heavy quark and decay electron quenching if the quark  $p_T$  is rescaled by a factor of  $\sim 2$ .

In Fig. 3, the sensitivity of the electron quenching to variations in the heavy quark fragmentation scheme is shown by the difference between the solid and dashed curves. The solid curves are calculated as in Ref. [34] while the dashed curves arise when Peterson fragmentation ( $\epsilon_c = 0.06, \epsilon_b = 0.006$ ) is used. While there can be considerable differences in the fragmentation schemes on an absolute scale, see Fig. 4, these differences mostly cancel in the nuclear modification factors shown in Fig. 3.

The yellow band corresponding to the combined  $c+b \rightarrow e$  electron sources shows that, in the kinematic range  $4 < p_T(e) < 10$  GeV accessible at RHIC,  $R_{AA}(e)$  is dominated by  $b$  quark quenching. Even for the highest opacity, shown on the right-hand side, we therefore predict that due to the  $b \rightarrow e$  contribution

$$R_{AA}(e) > 0.5 \text{ for } p_T < 6 \text{ GeV} . \quad (3)$$

Increasing the opacity further is not an option within the theory of radiative energy loss because pion quenching would then be over-predicted.

The robustness of the bottom dominance in the electron spectrum can be seen in the ratio of charm relative to bottom decays to electrons in Fig. 4. We use the NLO MNR code [35] to compute heavy quark production for a range of mass and scale values:  $1.2 < m_c < 1.7$  GeV,  $4.5 < m_b < 5$  GeV and combinations of the renormalization,  $\mu_R$ , and factorization,  $\mu_F$ , scales such that  $(\mu_R/m_T, \mu_F/m_T) = (1, 1), (2, 1), (1, 2)$  and  $(2, 2)$ . We employ the same  $(\mu_R/m_T, \mu_F/m_T)$  combinations for both charm and bottom to maintain the asymptotic approach of the distributions at high  $p_T$ . In all cases, the bottom contribution becomes larger for  $p_T < 5.5$  GeV, even before energy loss is applied. Changing the Peterson function parameter,  $\epsilon_Q$ , from the standard values of  $\epsilon_c = 0.06$  and  $\epsilon_b = 0.006$  to the more delta-function like values of  $\epsilon_c = \epsilon_b = 10^{-5}$  shifts the cross over to higher  $p_T$ , more similar to the results with the FONLL fragmentation scheme. No reasonable variations of the parameters controlling fragmentation of heavy quarks can make the bottom contribution to electrons negligible at RHIC.

As a final check, in Fig. 5 we show the “electron reach” defined by the transverse momentum distribution of the initial heavy quarks that decay to electrons with  $p_T = 5 - 6$  GeV. As can be readily seen, this range of electron  $p_T$  is sensitive to heavy quark quenching at approximately twice this scale:  $p_T \sim 6 - 10$  GeV with hard fragmentation parameters,  $\epsilon_c = \epsilon_b = 10^{-5}$ , and  $p_T \sim 9 - 14$  for the standard Peterson parameters. Given the slow variation of heavy quark quenching in the  $p_T \sim 10 - 20$  GeV range seen in Fig. 2, it is easy to understand why single electron quenching is robust to uncertainties in the

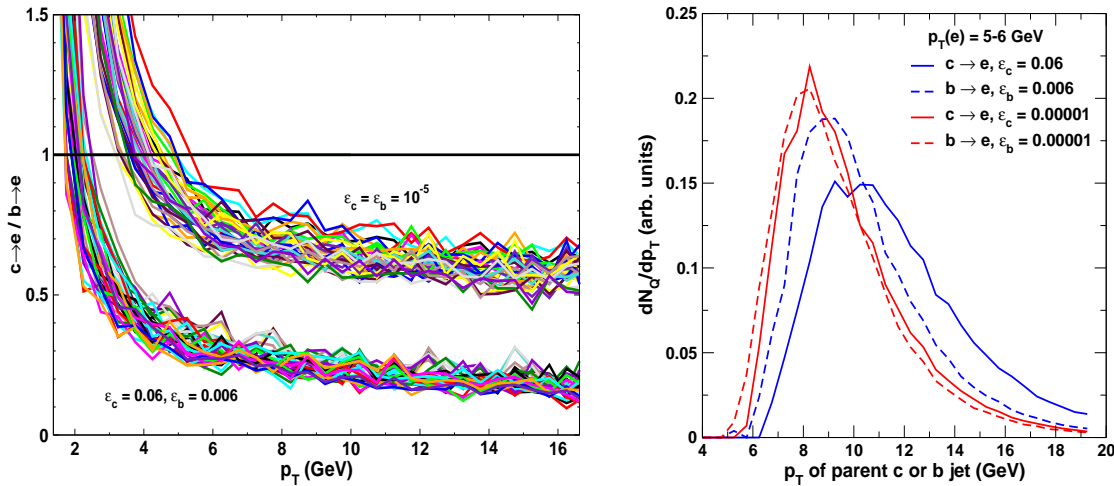


FIG. 4: [left] The ratio of charm to bottom decays to electrons obtained by varying the quark mass and scale factors. The effect of changing the Peterson function parameters from  $\epsilon_c = 0.06$ ,  $\epsilon_b = 0.006$  (lower band) to  $\epsilon_c = \epsilon_b = 10^{-5}$  (upper band) is also illustrated.

FIG. 5: [right] The electron reach, defined by the distribution of initial  $c$  and  $b$  quark momenta that after fragmentation and decay produce an electron with  $p_T = 5 - 6$  GeV using the PYTHIA fragmentation scheme.

heavy quark fragmentation scheme, as shown in Fig. 3.

#### Conclusions.

In this letter we predicted the nuclear modification factor of single electrons,  $R_{AA}(p_T, m_Q, dN_g/dy)$ , produced by fragmentation of quenched bottom as well as charm quark jets in central Au+Au collisions with  $\sqrt{s} = 200$  AGeV. We found that within the DGLV theory of radiative energy loss,  $b$  quark jets give the dominant contribution to  $p_T \sim 5$  GeV electrons, limiting  $R_{AA}(e) > 0.5$ . Therefore, if the preliminary PHENIX data suggesting  $R_{AA}(e) < 0.5$  are confirmed, it will be a theoretical challenge to devise novel energy loss mechanisms that make

the sQGP opaque to bottom quarks of  $p_T \sim 10 - 20$  GeV without over-predicting the observed light hadron quenching in the  $p_T \sim 10$  GeV range.

**Acknowledgments:** Valuable discussions with Azfar Adil, Brian Cole, John Harris, William Horowitz, Denes Molnar, Thomas Ullrich, Ivan Vitev and Nu Xu are gratefully acknowledged. This work is supported by the Director, Office of Science, Office of High Energy and Nuclear Physics, Division of Nuclear Physics, of the U.S. Department of Energy under Grants No. DE-FG02-93ER40764, DE-AC02-05CH11231.

- 
- [1] BRAHMS, PHOBOS, STAR, and PHENIX Collaborations, “First Three Years of Operations at RHIC”, BNL-73847-2005 Formal Report, Nucl. Phys. A **757**, 184 (2005), pp. 1, 28, 102, 184.
- [2] [http://www.bnl.gov/bnlweb/pubaf/pr/PR\\_display.asp?prID=05-38](http://www.bnl.gov/bnlweb/pubaf/pr/PR_display.asp?prID=05-38)
- [3] E. Shuryak, Prog. Part. Nucl. Phys. **53**, 273 (2004) [arXiv:hep-ph/0312227]; D. Teaney, J. Lauret and E. V. Shuryak, Phys. Rev. Lett. **86**, 4783 (2001) [arXiv:nucl-th/0011058].
- [4] P. F. Kolb and U. W. Heinz, Quark Gluon Plasma 3, (ed. R.C. Hwa and X.N. Wang, World Scientific, Singapore) pp. 634-714, arXiv:nucl-th/0305084; P. F. Kolb, P. Huovinen, U. W. Heinz and H. Heiselberg, Phys. Lett. B **500**, 232 (2001) [arXiv:hep-ph/0012137].
- [5] T. Hirano and M. Gyulassy, [arXiv:nucl-th/0506049]
- [6] M. Gyulassy, I. Vitev, X. N. Wang and B. W. Zhang, Quark Gluon Plasma 3, (ed. R.C. Hwa and X.N. Wang, World Scientific, Singapore) pp. 123-191; nucl-th/0302077; A. Kovner and U. Wiedemann, pp. 192-248 op cit. [arXiv:hep-ph/0304151]; P. Jacobs and X. N. Wang, Prog. Part. Nucl. Phys. **54**, 443 (2005) [arXiv:hep-ph/0405125]. X. N. Wang and M. Gyulassy, Phys. Rev. Lett. **68**, 1480 (1992).
- [7] M. Gyulassy, P. Levai and I. Vitev, Nucl. Phys. B **594**, 371 (2001) [arXiv:nucl-th/0006010].
- [8] M. Gyulassy, P. Levai and I. Vitev, Phys. Lett. B **538**, 282 (2002) [arXiv:nucl-th/0112071].
- [9] I. Vitev and M. Gyulassy, Phys. Rev. Lett. **89**, 252301 (2002) [arXiv:hep-ph/0209161];
- [10] “New Discoveries at RHIC - the current case for the strongly interactive QGP”, Proc. RBRC Workshop, May 14-15, 2004, BNL-72391-2004, Nucl. Phys. A **750**, 1 (2005).
- [11] Yu. L. Dokshitzer and D. E. Kharzeev Phys. Lett. B **519**, 199 (2001) [arXiv:hep-ph/0106202].

- [12] M. Djordjevic and M. Gyulassy, Nucl. Phys. A **733**, 265 (2004) [arXiv:nucl-th/0310076].
- [13] M. Djordjevic and M. Gyulassy, Phys. Rev. C **68**, 034914 (2003) [arXiv:nucl-th/0305062].
- [14] M. Djordjevic and M. Gyulassy, Phys. Lett. B **560**, 37 (2003) [arXiv:nucl-th/0302069].
- [15] M. Djordjevic, M. Gyulassy and S. Wicks, Phys. Rev. Lett. **94**, 112301 (2005) [arXiv:hep-ph/0410372].
- [16] B. W. Zhang, E. Wang and X. N. Wang, Phys. Rev. Lett. **93**, 072301 (2004) [arXiv:nucl-th/0309040].
- [17] N. Armesto, A. Dainese, C. A. Salgado and U. A. Wiedemann, Phys. Rev. D **71**, 054027 (2005) [arXiv:hep-ph/0501225].
- [18] K. J. Eskola, H. Honkanen, C. A. Salgado and U. A. Wiedemann, Nucl. Phys. A **747**, 511 (2005) [arXiv:hep-ph/0406319].
- [19] J. W. Harris, arXiv:nucl-ex/0504023.
- [20] K. Adcox *et al.* [PHENIX Collaboration], Phys. Rev. Lett. **88**, 192303 (2002) [arXiv:nucl-ex/0202002].
- [21] J. Adams *et al.* [STAR Collaboration], Phys. Rev. Lett. **94**, 062301 (2005) [arXiv:nucl-ex/0407006].
- [22] S. S. Adler *et al.* [PHENIX Collaboration], Phys. Rev. Lett. **94**, 082301 (2005) [arXiv:nucl-ex/0409028].
- [23] S. S. Adler *et al.* [PHENIX Collaboration], arXiv:nucl-ex/0502009.
- [24] F. Laue [STAR Collaboration], J. Phys. G **31**, S27 (2005) [arXiv:nucl-ex/0411007].
- [25] R. Averbek, arXiv:nucl-ex/0505018.
- [26] X. y. Lin, arXiv:hep-ph/0412124.
- [27] Xin Dong, Ph.D. thesis, Univ. Sci. Tech. China, Hefei 2005 (unpublished); Nu Xu, private communication.
- [28] D. Molnar, J. Phys. G **31**, S421 (2005) [arXiv:nucl-th/0410041]; arXiv:nucl-th/0503051.
- [29] B. Zhang, L. W. Chen and C. M. Ko, arXiv:nucl-th/0502056.
- [30] H. van Hees and R. Rapp, Phys. Rev. C **71**, 034907 (2005) [arXiv:nucl-th/0412015].
- [31] G. D. Moore and D. Teaney, arXiv:hep-ph/0412346.
- [32] D. Molnar and M. Gyulassy, Nucl. Phys. A **697**, 495 (2002) [Erratum-ibid. A **703**, 893 (2002)] [arXiv:nucl-th/0104073].
- [33] W. Horowitz, M. Gyulassy and D. Molnar, in preparation.
- [34] M. Cacciari, P. Nason and R. Vogt, arXiv:hep-ph/0502203.
- [35] M. L. Mangano, P. Nason and G. Ridolfi, Nucl. Phys. B **373**, 295 (1992).
- [36] R. Vogt, Int. J. Mod. Phys. E **12**, 211 (2003) [arXiv:hep-ph/0111271].
- [37] J. Pumplin, D. R. Stump, J. Huston, H. L. Lai, P. Nadolsky and W. K. Tung, JHEP **0207**, 012 (2002) [arXiv:hep-ph/0201195]; D. Stump, J. Huston, J. Pumplin, W. K. Tung, H. L. Lai, S. Kuhlmann and J. F. Owens, arXiv:hep-ph/0303013.
- [38] M. Cacciari and P. Nason, Phys. Rev. Lett. **89**, 122003 (2002) [arXiv:hep-ph/0204025].
- [39] M. Cacciari, S. Frixione, M. L. Mangano, P. Nason and G. Ridolfi, JHEP **0407**, 033 (2004) [arXiv:hep-ph/0312132].
- [40] M. Cacciari and P. Nason, JHEP **0309**, 006 (2003) [arXiv:hep-ph/0306212].
- [41] E. Braaten, K. Cheung, S. Fleming and T. C. Yuan, Phys. Rev. D **51**, 4819 (1995) [arXiv:hep-ph/9409316].
- [42] V. G. Kartvelishvili, A. K. Likhoded and V. A. Petrov, Phys. Lett. B **78**, 615 (1978).
- [43] B. Aubert *et al.* [BABAR Collaboration], Phys. Rev. D **69**, 111104 (2004) [arXiv:hep-ex/0403030].
- [44] A. H. Mahmood *et al.* [CLEO Collaboration], Phys. Rev. D **70**, 032003 (2004) [arXiv:hep-ex/0403053].
- [45] J. Yelton [CLEO Collaboration], <http://www.lns.cornell.edu/public/TALK/2004/TALK04-42/>.
- [46] S. Eidelman *et al.* [Particle Data Group Collaboration], Phys. Lett. B **592**, 1 (2004).
- [47] T. Sjostrand *et al.*, Comput. Phys. Commun. **135**, 238 (2001) [arXiv:hep-ph/0010017].
- [48] C. Peterson, D. Schlatter, I. Schmitt and P. M. Zerwas Phys. Rev. D **27**, 105 (1983).
- [49] B.G. Zakharov, JETP Lett. **76**, 201 (2002) [arXiv:hep-ph/0207206].
- [50] M. Djordjevic, M. Gyulassy and S. Wicks, Euro Phys. J C, in press (2005); M. Djordjevic, Columbia University Ph.D. Thesis 2005 (unpublished).
- [51] M. Gyulassy, I. Vitev, X. N. Wang and P. Huovinen, Phys. Lett. B **526**, 301 (2002) [arXiv:nucl-th/0109063].
- [52] S. S. Adler *et al.* [PHENIX Collaboration], Phys. Rev. Lett. **91**, 072301 (2003) [arXiv:nucl-ex/0304022].
- [53] I. Vitev, Phys. Lett. B **606**, 303 (2005) [arXiv:nucl-th/0404052].
- [54] A. Adil and M. Gyulassy, Phys. Lett. B **602** (2004) 52 [arXiv:nucl-th/0405036].